Electronic Supplementary Material (ESI) for Analyst.

Supplementary Information

Triple Ligation-based Formation of G-quadruplex for Simultaneous Detection of Multiple miRNAs

Kazi Morshed Alom, Young Jun Seo*

Department of Chemistry, Jeonbuk National University, Jeonju 561-756, Republic of Korea

Tel.: +82-63-270-3417; Fax: +82-63-270-3408; E-mail: yseo@jbnu.ac.kr

Oligonucleotide name	Oligonucleotide sequence
MLP1 (duplex)	5’ [Phosphate]- **CTG ATA AGC TA**C CCT ATA GTG AGT CGT ATT A TTA CCC ACC CTA CCC ACC CTC **A TC ACA AGT TAG** -3' + 5’ TAA TAC GAC TCA CTA TAG GG -3’
MLP2	5' [Phosphate]- **TTC AGT TCT CA**G TCA AGT TAC **TCA ACA TCA GT** -3'
MLP3	5' [Phosphate]- **GGT CTC AGG GA**A TCG TGA GAC **AAC CCA TGG AA** -3'
MLP1’ (duplex)	5’ [Phosphate]- **CTG ATA AGC TA**C CCT ATA GTG AGT CGT ATT A **A TC ACA AGT TAG** -3' + 5’ TAA TAC GAC TCA CTA TAG GG -3’

Table S1. Multiple ligation-based padlock probe sequences used for the system.

Oligonucleotide name	Oligonucleotide sequence
Target 1 (miRNA 21)	5′- UAG CUU AUC AGA CUG AUG UUG A -3′
Target 1 (1 mismatch)	5′- UAG CUU AUC A**C**A CUG AUG UUG A -3′
Target 1 (2 mismatch)	5′- UAG CUU AUC A**C**A **U**UG AUG UUG A -3′
Target 1 (3 mismatch)	5′- UAG CUU AU**G** A**C**A **U**UG AUG UUG A -3′
Target 2 (miRNA 146a)	5′- UGA GAA CUG AAU UCC AUG GGU U -3′
Target 2 (1 mismatch)	5′- UGA GAA CUG A**G**U UCC AUG GGU U -3′
Target 2 (2 mismatch)	5′- UGA GAA CUG A**G**U **G**CC AUG GGU U -3′
Target 2 (3 mismatch)	5′- UGA GAA CU**A** A**G**U **G**CC AUG GGU U -3′
Target 3 (miRNA 25b)	5′- UCC CUG AGA CCC UAA CUU GUG A -3′
Target 3 (1 mismatch)	5′- UCC CUG AGA C**A**C UAA CUU GUG A -3′
Target 3 (2 mismatch)	5′- UCC CUG AGA C**A**C **G**AA CUU GUG A -3′
Target 3 (3 mismatch)	5′- UCC CUG AG**G** C**A**C **G**AA CUU GUG A -3′
miR24-3p	5′- UGG CUC AGU UCA GCA GGA ACA G -3′

Table S2. Targets along with their mismatch sequences used for the selectivity analysis.

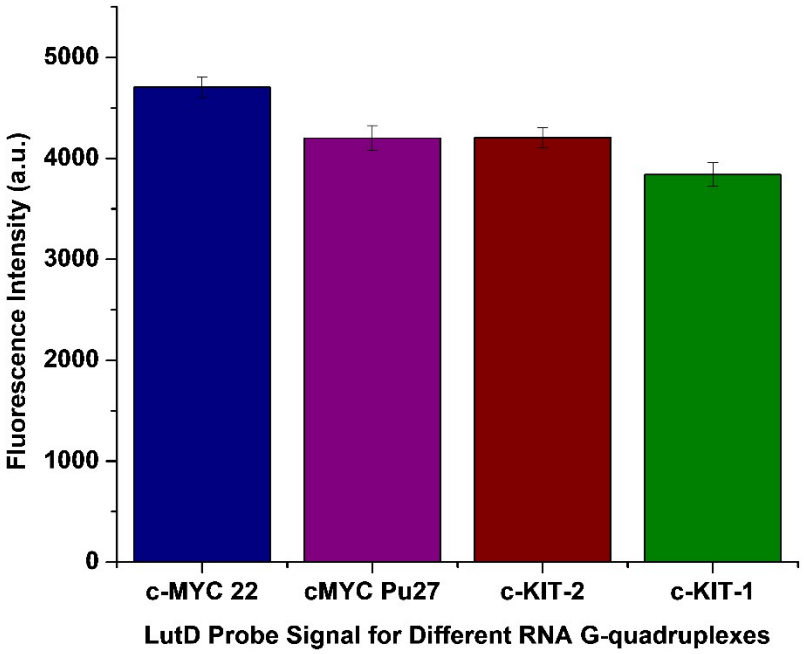

Figure S1. Bar diagram to compare the intensity of the fluorescence signal produced by different RNA G-quadruplexes. Error bars represent the standard deviation of three different samples.

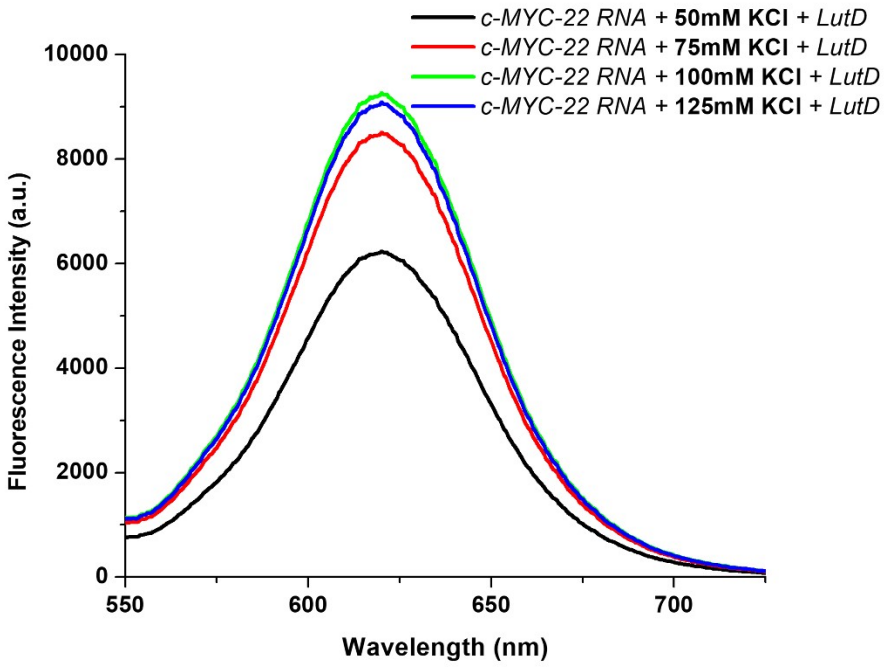

Figure S2. Effect of different KCl concentrations on the intensity of the fluorescence emission of LutD.

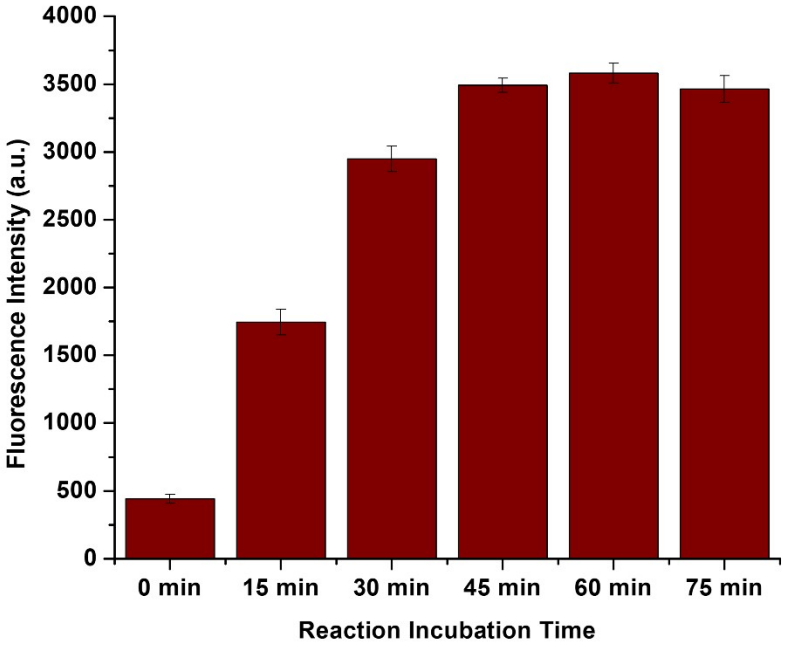

Figure S3. Bar diagram to visualize the effect of the incubation time on the fluorescence signal to determine the shortest incubation time required to achieve the highest intensity fluorescence signal. Error bars represent the standard deviation of three different samples.

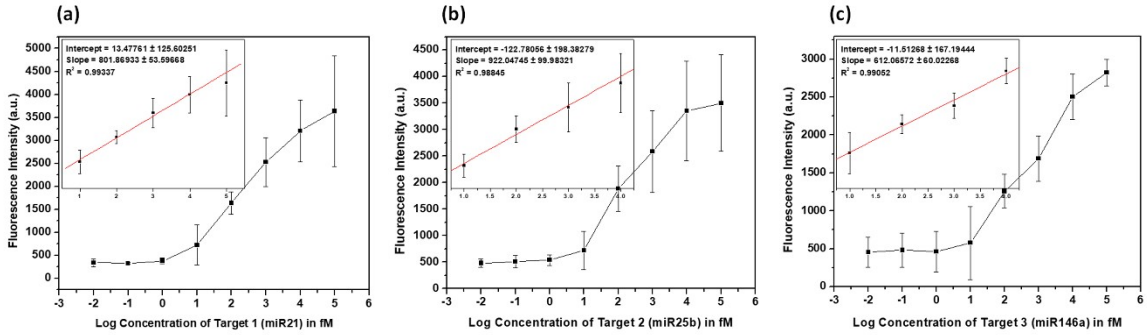

Figure S4. a., b. & c. Plot representing the deviation of the signal intensity of 3 different miRNAs in 10% human serum for diluting concentrations. The error bar represents the standard deviation of three different spiked samples.

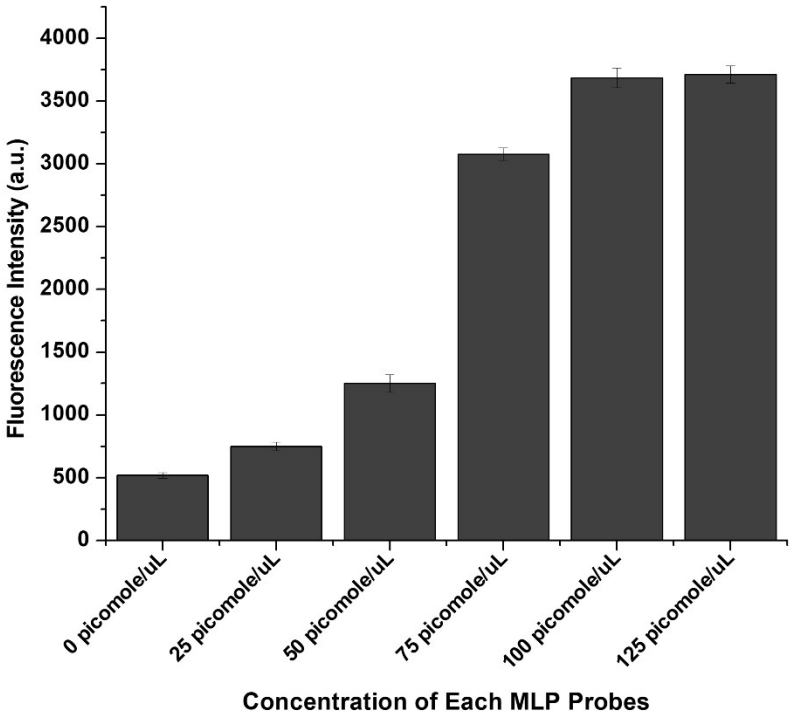

Figure S5. Bar diagram for analysis of the MLP probe concentration required for the system. Error bars represent the standard deviation of three different samples.

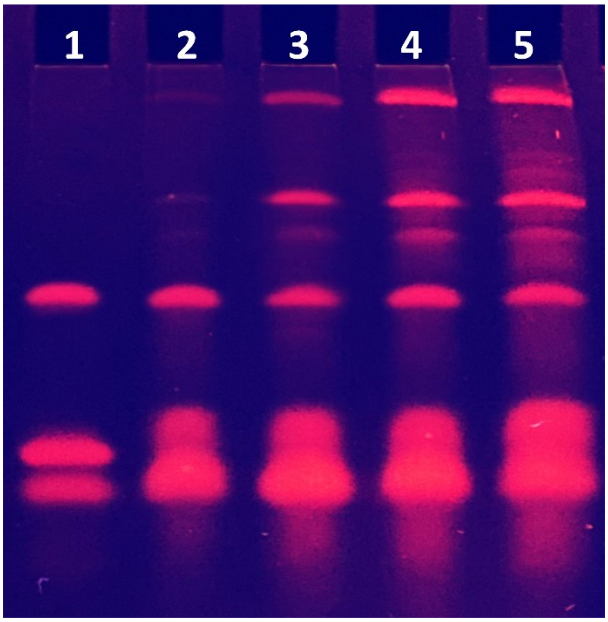

Figure S6. 16% denaturing PAGE for optimization of the ligation analyzed by varying the SplintR ligase concentrations. Lane 1: MLP probes + Target (1 + 2 + 3) + SplintRL 0 Unit; lane 2: : MLP probes + Target (1 + 2 + 3) + SplintRL 6.25 Unit; lane 3: MLP probes + Target (1 + 2 + 3) + SplintRL 12.5 Unit; lane 4: : MLP probes + Target (1 + 2 + 3) + SplintRL 25 Unit; lane 5: : MLP probes + Target (1 + 2 + 3) + SplintRL 50 Unit.

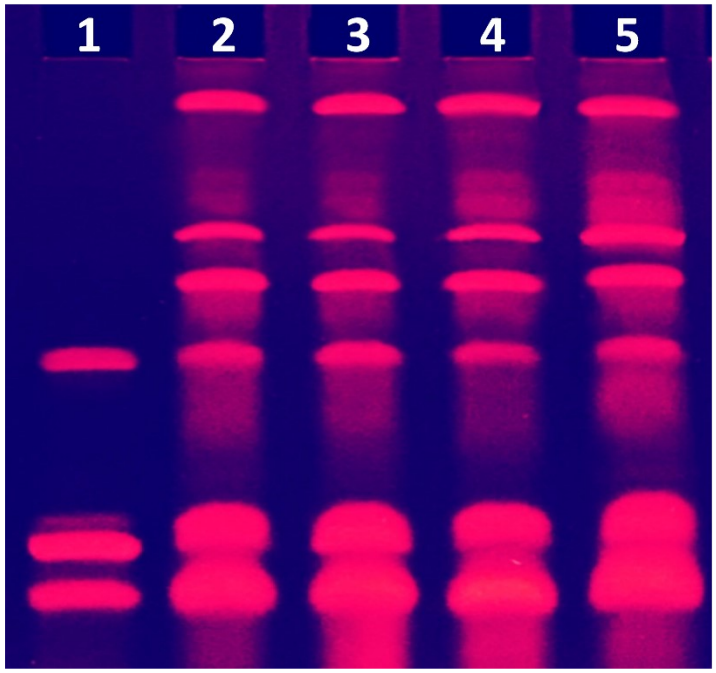

Figure S7. 16% denaturing PAGE analyzing the effect of target sequence changes on ligation efficiency. Lane 1: MLP probes + Target (1 + 2 + 3); lane 2: MLP probes + Target (1_sequence changed + 2 + 3) + SplintRL; lane 3: MLP probes + Target (1 + 2_sequence changed + 3) + SplintRL; lane 4: MLP probes + Target (1 + 2 + 3_sequence changed) + SplintRL; lane 5: MLP probes + Target (1 + 2 + 3) + SplintRL.

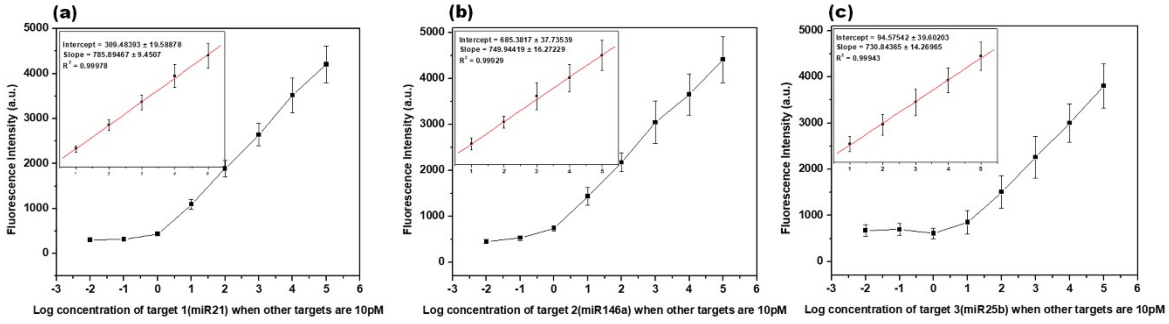

Figure S8. a., b. & c. Plot presenting the deviation of the signal intensity for each miRNA target when other targets are present in 10 pM concentrations. The limit of detection (LOD) for target 1 (miR21), target 2 (146a), and target 3 (25b) was found respectively 1.38 fM, 1.93 fM, and 2.04 fM. The error bar represents the standard deviation of three different samples.

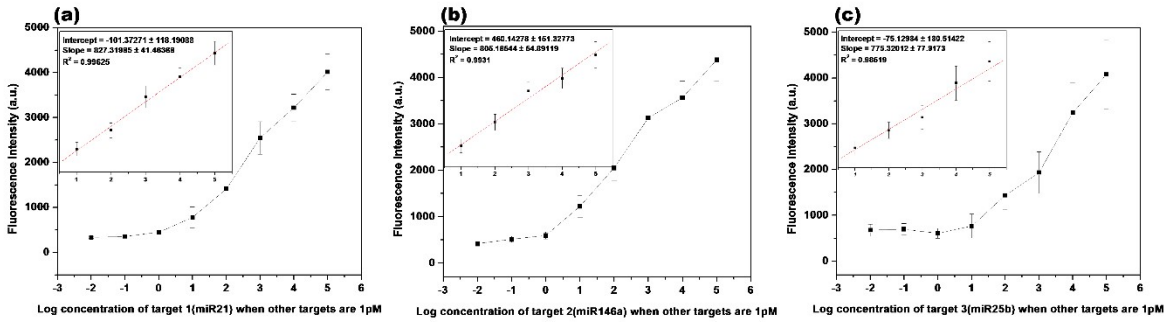

Figure S9. a., b. & c. Plot presenting the deviation of the signal intensity for each miRNA target when other targets are present in 1 pM concentrations. The limit of detection (LOD) for target 1 (miR21), target 2 (146a), and target 3 (25b) was found respectively 6.55 fM, 11.86 fM, and 21.41 fM. The error bar represents the standard deviation of three different samples.

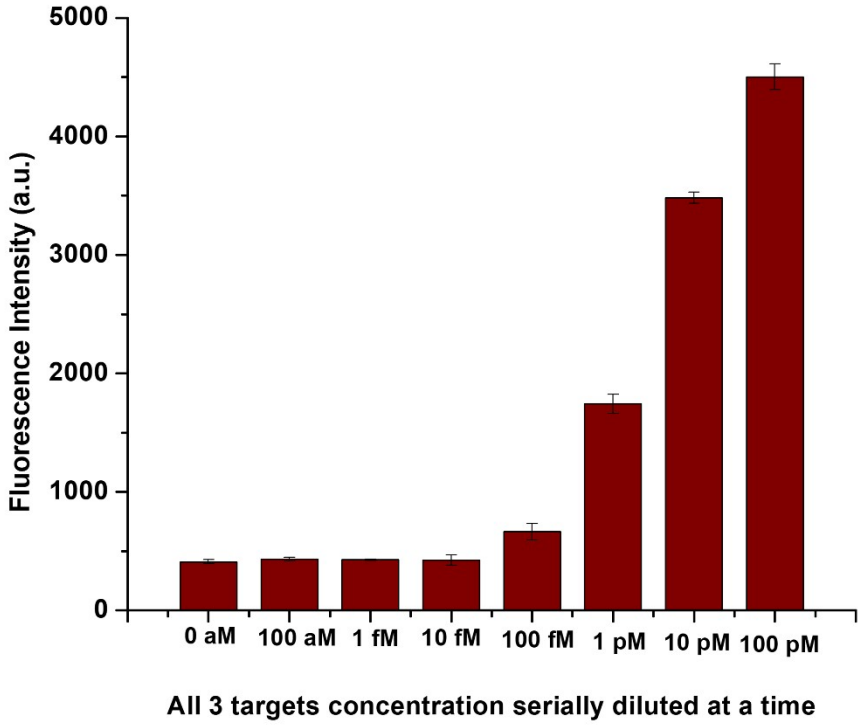

Figure S10. Bar diagram representing the limit of detection when all three miRNA targets are equally diluted at the same time. The data shows that for dilution of each miRNA until 100 fM concentration, the signal could be differentiated compared to samples with no target. The error bar represents the standard deviation of three different samples.

Analytical method	Reaction method	miRNA targets	Limit of detection (LOD)	Linear range	Detection time (in minutes)	Ref.
SERS	DNA-conjugated F-AuNPs and AgMNPs	miR-122, miR-223, miR-21	349 aM, 374 aM, 311 aM	1 fM to 10 nM	150	[1]
Microscopy	DNA-PAINT imaging using DNA origami nanoarray system	miR-153, miR-21, miR-142, let-7a	11 fM, 388 fM, 17 fM, 150 fM	Up to 10 nM	60	[2]
HPLC	DSN-mediated target recycling	miR-122, miR-155, miR-21	0.39 fM, 0.30 fM, 0.26 fM	1 fM to 100 pM	210	[3]
Electrochemical	TBAPy-MA-COF-based recyclable aptasensor	miR- 155, miR- 122	6.7 fM, 1.5 fM	0.01–1000 pM	30	[4]
Fluoremetric	FRET with dual colored Au NCs as energy donors	miR-21, let-7a	4.2 pM, 3.6 pM	0.01–2.0 nM, 0.01–2.5 nM	60	[5]
Fluoremetric	Multiple ligation coupled with G-quadruplex sensing	miR-21, miR-146a, miR-25b	1.13 fM, 1.37 fM, 1.51 fM	1 fM to 100 pM	45	This work

Table S3. Comparision of the proposed system with some other reported systems.

References

1 J. Wu, X. Zhou, P. Li, X. Lin, J. Wang, Z. Hu, P. Zhang, D. Chen, H. Cai, R. Niessner, C. Haisch, P. Sun, Y. Zheng, Z. Jiang and H. Zhou, *Anal Chem*, 2021, **93**, 8799–8809.

2 S. Kocabey, G. Chiarelli, G. P. Acuna and C. Ruegg, *Biosens Bioelectron*, 2023, **224**, 115053.

3 T. Qi, C. Song, J. He, W. Shen, D. Kong, H. Shi, L. Tan, R. Pan, S. Tang and H. K. Lee, *Anal Chem*, 2020, **92**, 5033–5040.

4 Z. Cao, F. Duan, X. Huang, Y. Liu, N. Zhou, L. Xia, Z. Zhang and M. Du, *Anal Chim Acta*, 2019, **1082**, 176–185.

5 S. Xu, Y. Nie, L. Jiang, J. Wang, G. Xu, W. Wang and X. Luo, *Anal Chem*, 2018, **90**, 4039–4045.